Cell

Inhibition of mTORC1 by Astrin and Stress Granules Prevents Apoptosis in Cancer Cells

Kathrin Thedieck,[1,2,3,4,14,15,*] Birgit Holzwarth,[1,2,14] Mirja Tamara Prentzell,[1,2,5] Christopher Boehlke,[8] Kathrin Kläsener,[1,3,9] Stefanie Ruf,[1,2,3,6] Annika Gwendolin Sonntag,[1,2] Lars Maerz,[1,2] Sushma-Nagaraja Grellscheid,[10] Elisabeth Kremmer,[11] Roland Nitschke,[1,3,4] E. Wolfgang Kuehn,[3,8] Johan W. Jonker,[13] Albert K. Groen,[13] Michael Reth,[1,3,9] Michael N. Hall,[12] and Ralf Baumeister[1,2,3,4,7]

[1]Faculty of Biology
[2]Bioinformatics and Molecular Genetics, Faculty of Biology
[3]BIOSS Centre for Biological Signalling Studies
[4]Center for Systems Biology (ZBSA)
[5]Spemann Graduate School of Biology and Medicine (SGBM)
[6]Research Training Group (RTG) 1104
[7]ZBMZ Center for Biochemistry and Molecular Cell Research, Faculty of Medicine
Albert-Ludwigs-University Freiburg, 79104 Freiburg, Germany
[8]Renal Division, University Hospital Freiburg, 79106 Freiburg, Germany
[9]Molecular Immunology, Max-Planck Institute of Immunobiology and Epigenetics, 79108 Freiburg, Germany
[10]School of Biological and Biomedical Sciences, Durham University, Durham DH1 3LE, UK
[11]Helmholtz Zentrum München, Institute of Molecular Immunology, 81377 Munich, Germany
[12]Biozentrum, University of Basel, Klingelbergstrasse 50/70, 4056 Basel, Switzerland
[13]Center for Liver, Digestive and Metabolic Diseases, Department of Pediatrics, University of Groningen, University Medical Center Groningen, Hanzeplein 1, 9713 GZ Groningen, The Netherlands
[14]These authors contributed equally to this work
[15]Present address: Center for Liver, Digestive and Metabolic Diseases, Department of Pediatrics, University of Groningen, University Medical Center Groningen, Hanzeplein 1, 9713 GZ Groningen, The Netherlands
*Correspondence: k.thedieck@umcg.nl
http://dx.doi.org/10.1016/j.cell.2013.07.031

SUMMARY

Mammalian target of rapamycin complex 1 (mTORC1) controls growth and survival in response to metabolic cues. Oxidative stress affects mTORC1 via inhibitory and stimulatory inputs. Whereas downregulation of TSC1-TSC2 activates mTORC1 upon oxidative stress, the molecular mechanism of mTORC1 inhibition remains unknown. Here, we identify astrin as an essential negative mTORC1 regulator in the cellular stress response. Upon stress, astrin inhibits mTORC1 association and recruits the mTORC1 component raptor to stress granules (SGs), thereby preventing mTORC1-hyperactivation-induced apoptosis. In turn, balanced mTORC1 activity enables expression of stress factors. By identifying astrin as a direct molecular link between mTORC1, SG assembly, and the stress response, we establish a unifying model of mTORC1 inhibition and activation upon stress. Importantly, we show that in cancer cells, apoptosis suppression during stress depends on astrin. Being frequently upregulated in tumors, astrin is a potential clinically relevant target to sensitize tumors to apoptosis.

INTRODUCTION

The mammalian target of rapamycin (mTOR) kinase is a central regulator of growth and metabolism (Polak and Hall, 2009; Laplante and Sabatini, 2012). mTOR occurs in two multiprotein complexes, mTOR complex 1 (mTORC1), containing the specific binding proteins raptor and PRAS40, and mTORC2 containing rictor and other binding partners. mTORC1 responds to insulin and amino acids (aa) to control growth and protein homeostasis via translation and autophagy. mTORC1 has been also reported to respond to redox stress (Bae et al., 1999; Huang et al., 2002), but the interplay of inhibitory and activating redox inputs, as well as the molecular identity of inhibitory redox signals and their relevance for cellular stress survival, remain unclear.

In contrast, the mechanisms of mTORC1 induction by insulin and aa are relatively well understood. In response to aa, the rag GTPases induce mTORC1-translocation to lysosomes. Here, mTORC1 can be further activated by insulin via the insulin receptor (IR) and the insulin-receptor-substrate (IRS), which activates class I-phosphoinositide 3-kinases (PI3K). PI3K enables

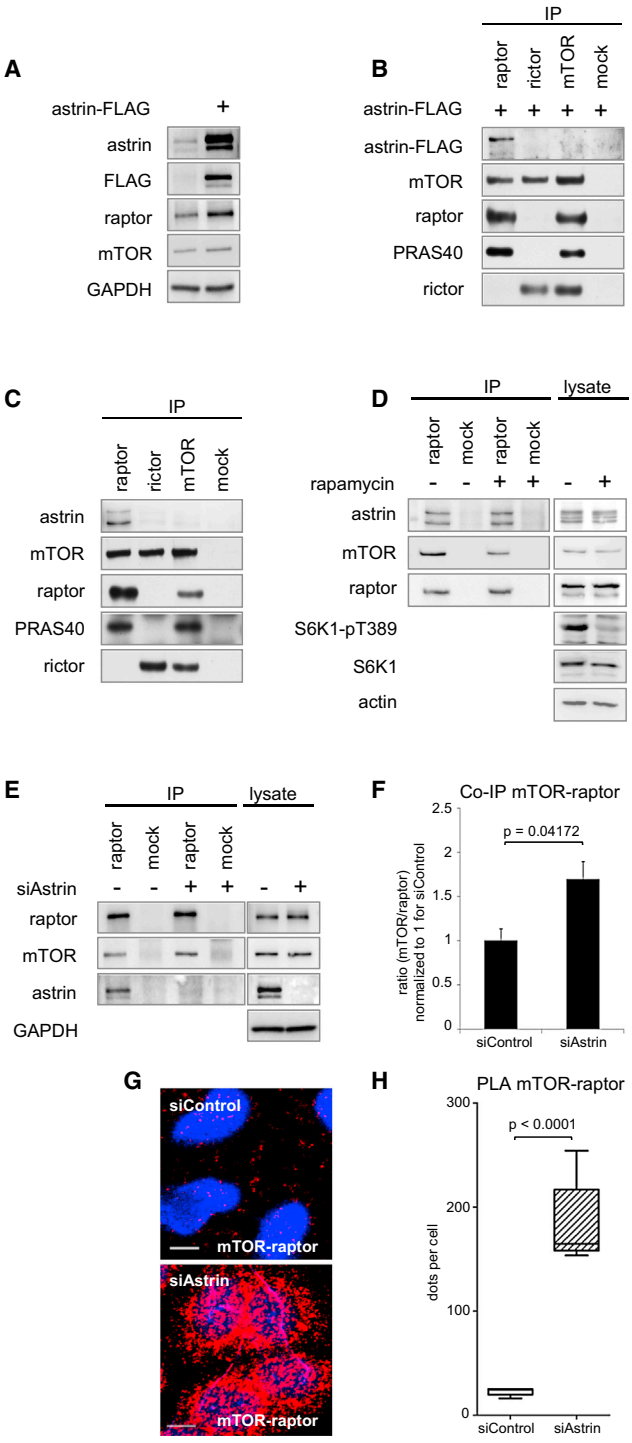

Figure 1. Astrin Binds to Raptor and Prevents mTORC1 Assembly

(A) Astrin-FLAG overexpression induces raptor levels.

(B) Astrin-FLAG coimmunoprecipitates with raptor, but not with mTOR or rictor.

(C) Endogenous astrin coimmunoprecipitates with raptor, but not with mTOR or rictor.

(D) Rapamycin does not alter raptor-astrin binding.

(E) Astrin siRNA induces mTOR-raptor co-IP.

(F) Relative quantitation of mTOR co-IP with raptor (E). Ratio mTOR/raptor for n = 5 experiments. Data normalized to 1 for siControl, and represented as mean ± SEM.

(G) Astrin siRNA induces mTOR-raptor association in situ. Nuclei were stained with DAPI (blue), and PLA was performed for raptor and mTOR (red).

(H) Relative quantitation of mTORC1 assembly in situ without and with astrin siRNA (G). Dots/cell on control and astrin siRNA slides. Data represented as median, 25th–75th percentile (box), 5th–95th percentile (whiskers). See Figure S1C for quantitation of fluorescence intensity.

Experiments performed in HeLa cells. Data representative of at least three independent experiments. See also Figure S1.

Akt-T308 phosphorylation by phosphoinositide-dependent protein kinase 1 (PDK1). Akt inhibits the tuberous sclerosis complex 1/2 (TSC1-TSC2) dimer, which is the inhibitory GTPase-activating protein for the small GTPase Rheb. The best characterized mTORC1 substrates are ribosomal protein S6 kinase 1 (S6K1), the 4E-binding protein 4E-BP1, and PRAS40. A negative-feedback loop (NFL) inhibits PI3K-Akt signaling upon mTORC1 activation. This NFL is mediated via IRS phosphorylation by S6K1 and Grb10 phosphorylation by mTORC1.

Under oxidative stress, downregulation of the TSC1-TSC2 complex mediates mTORC1 activation (Yoshida et al., 2011), whereas AMP-activated protein kinase (AMPK) activation (Mihaylova and Shaw, 2011) inhibits mTORC1 (Alexander et al., 2010; Li et al., 2010). Recent evidence suggests that stress granules (SGs) also play a role in inhibition of mTOR (Luo et al., 2011; Takahara and Maeda, 2012; Talarek et al., 2010; Wippich et al., 2013). Oxidative stress induces SGs and P bodies (PBs) (Thomas et al., 2011). PBs are sites of mRNA decay, whereas SGs are sites of mRNA storage and triage during stress. SGs consist of monosomal nontranslating mRNAs and self-associating proteins, e.g., the RasGAP SH3-binding protein G3BP1, whose overexpression can be sufficient to induce SGs (Tourrière et al., 2003). SGs are also sites of translation initiation (Buchan and Parker, 2009), and SGs protect cells against apoptosis by sequestering signaling molecules (Arimoto et al., 2008).

In this study, we describe astrin as a novel raptor interactor that mediates mTORC1 inhibition under stress. We show that astrin is a critical component of mTORC1 signaling, coupling mTORC1 inhibition and SGs. We demonstrate that astrin inhibits mTOR-raptor association and recruits raptor to SGs to restrict mTORC1 activation upon metabolic challenge and redox stress. By preventing mTORC1 hyperactivation under stress, astrin mediates antiapoptotic SG functions. At the same time, TSC1-TSC2 controls astrin expression, and balanced mTORC1 activity is needed to enable expression of stress response proteins. Thus, we provide a unifying model in which loss of TSC1-TSC2 mediates mTORC1 activation by stress to allow stress factor expression, and astrin in a SG-dependent manner prevents mTORC1 hyperactivation to protect the cell from undergoing apoptosis.

RESULTS

Astrin Is a Specific Raptor Interactor which Inhibits mTORC1 Association

To identify novel mTOR regulators, we immunopurified endogenous mTOR, raptor, and rictor from HeLa cells and analyzed the

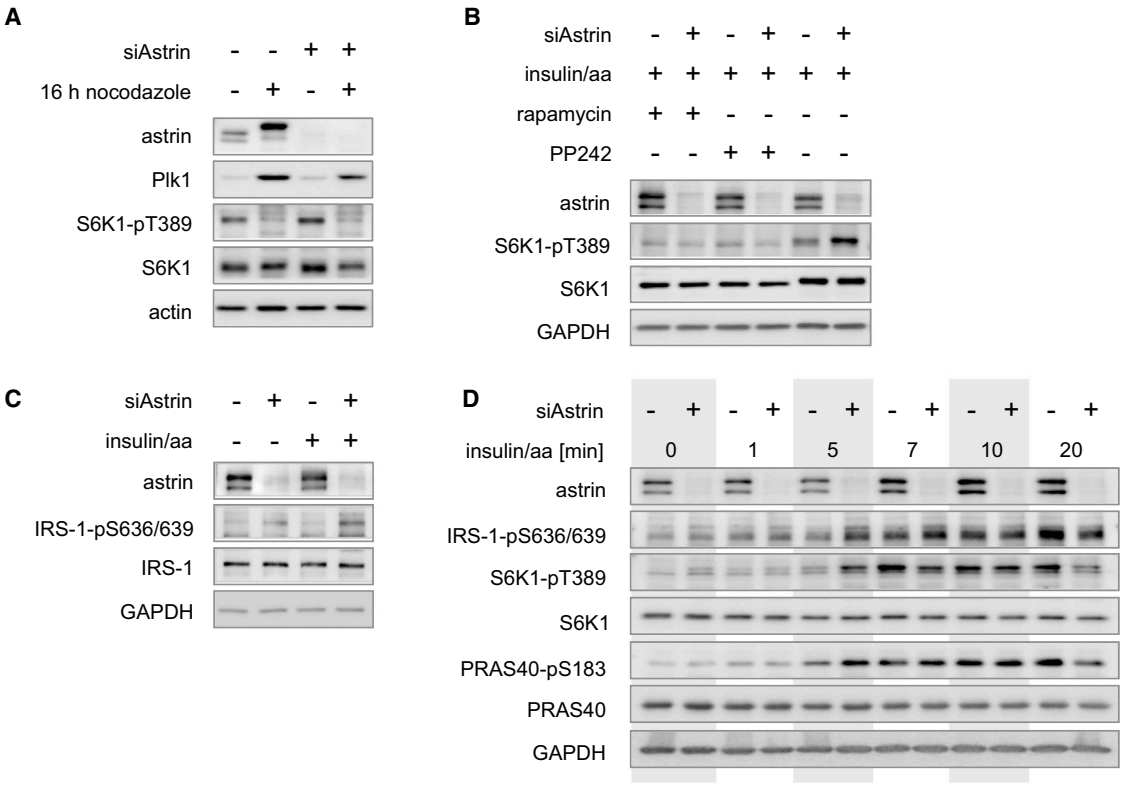

(legend on next page)

immunoprecipitates (IPs) by mass spectrometry (MS). We identified astrin in raptor IPs (Figure S1A available online), but not in mTOR or rictor IPs. This suggested that astrin binds to raptor, when the latter is not in a complex with mTOR.

Astrin (UniProtKB: Q96R06) has two isoforms of 160 and 140 kDa. High astrin mRNA levels correlate with negative prognosis in breast and lung cancer (Buechler, 2009; Välk et al., 2010). We analyzed astrin protein expression in three breast cancer cell lines. Astrin protein levels positively correlated with Akt activity, and negatively correlated with phosphorylation of the mTORC1 substrates PRAS40-S183 and S6K1-T389 (Figure S1B); raising the question whether astrin exerts an inhibitory effect on mTORC1.

To further analyze the astrin-raptor interaction, we overexpressed astrin-FLAG. Astrin-FLAG overexpression increased the level of raptor (Figure 1A). Furthermore, astrin-FLAG coimmunoprecipitated with raptor, but not with mTOR or rictor (Figure 1B), confirming our MS data. Also endogenous astrin coimmunopurified with raptor, but not with mTOR or rictor (Figure 1C). Thus, astrin is a specific interactor of the mTORC1 component raptor.

To test whether mTORC1 activity affects astrin-raptor association, we used the allosteric mTORC1 inhibitor rapamycin and followed astrin-raptor binding by co-IP. Expectedly, rapamycin inhibited S6K1 phosphorylation, and raptor dissociated from the mTOR-raptor-complex (Sarbassov et al., 2006), but no effect on astrin-raptor binding was observed (Figure 1D). Thus, mTORC1 inhibition does not affect raptor-astrin binding. In contrast, astrin inhibition affects mTORC1 assembly, as siRNA knockdown of astrin (siAstrin) resulted in increased mTOR amounts in raptor IPs (Figures 1E and 1F). To analyze the association of raptor with its binding partners by a complementary approach, we used proximity ligation assays (PLA) (Söderberg et al., 2008). PLA involves single-cell detection of two proximal proteins in situ. In contrast, IP results represent the average protein binding in several millions of lysed cells. The physiological environment and higher number of analyzed events may yield stronger observable effects in PLAs. We used PLA here, to the best of our knowledge for the first time, to analyze mTOR complex dynamics, and this approach revealed enhanced mTOR-raptor association upon astrin knockdown (Figures 1G and 1H), which appeared much stronger, as compared to IP. mTOR-raptor association in PLA was quantified by two different techniques (dot counting, Figure 1H, and overall intensity determination, Figure S1C), which yielded comparable results. We also tested whether astrin overexpression reduces mTOR-raptor binding (Figure S1D), but the increased raptor levels in astrin overexpressing cells did not allow a clear result. In contrast, siAstrin did not affect raptor levels (Figure 1E). Thus, based on increased mTOR-raptor association in siAstrin cells, measured by both IP and PLA, we conclude that astrin competes with mTOR for raptor binding, resulting in increased mTORC1 formation in the absence of astrin.

Astrin Inhibits mTORC1 Signaling

Astrin has been described as a regulator of mitotic progression (Chang et al., 2001; Gruber et al., 2002; Mack and Compton, 2001). mTORC1 has also been proposed to have a role in mitosis (Gwinn et al., 2010; Nakashima et al., 2008; Ramírez-Valle et al., 2010). We therefore tested whether astrin deficiency alters mTORC1 activity during mitosis. We arrested HeLa cells at G2/M with nocodazole and found that S6K1-T389 was only weakly phosphorylated and remained unaltered upon astrin knock down (Figure 2A). In contrast, astrin deficiency induced S6K1-pT389 in nonsynchronized cells (Figure 2A, lane 1 and 3, and Figure S2A, left), suggesting a regulatory role of astrin toward mTORC1 outside of mitosis. To rule out that astrin siRNA itself might increase the number of mitotic cells, we analyzed histone H3-S10 phosphorylation and polo-like-kinase 1 (Plk1) levels. None of these mitotic markers were induced by siAstrin (Figure S2B), consistent with findings of others (Halim et al., 2013). To ensure that astrin knockdown reproduces the described mitotic effects (Thein et al., 2007), we confirmed that also in our hands, nocodazole-induced histone H3-S10 phosphorylation was increased by astrin deficiency. We also tested five different shRNA clones against astrin and comparable results were obtained (Figure S2C). Of note, astrin-raptor binding was lost in nocodazole-arrested mitotic cells (Figure S2D), further pointing toward a function of the raptor-astrin complex outside of mitosis. We conclude that astrin deficiency in nonsynchronized cells induces phosphorylation of the mTORC1 substrate S6K1-T389, and this effect is independent of astrin's mitotic functions.

To further investigate the role of astrin in mTORC1 signaling, we examined insulin induction of mTORC1 in cells lacking astrin. Astrin knockdown enhanced S6K1-T389 phosphorylation (Figure 2B and S2A, right). The mTORC1-specific inhibitor rapamycin and the mTORC1/2 inhibitor PP242 (Benjamin et al., 2011), both potently inhibited S6K1-pT389 in astrin-deficient cells. Thus, astrin's inhibitory effect on S6K1-pT389 is mTORC1 dependent.

Figure 2. Astrin Deficiency Induces mTORC1 and a Negative-Feedback Loop toward the Insulin Receptor Substrate IRS-1

(A) Astrin deficiency does not alter S6K1 phosphorylation in mitotic cells but induces p70-S6K1-pT389 in nonsynchronized cultures. HeLa cells were synchronized at G2/M, or left nonsynchronized. See Figure S2A for relative quantitation of S6K1-T389 without and with siAstrin under basal conditions.

(B) Astrin-deficiency-induced S6K1 phosphorylation is inhibited by the mTOR inhibitors rapamycin and PP242. HeLa cells serum/aa starved; treated with PP242, rapamycin, or carrier (DMSO); and induced with insulin/aa.

(C) Astrin deficiency induces IRS-1 phosphorylation. Treatment as in Figure 2B.

(D) The dynamic of mTORC1 (S6K1 phosphorylation) induction and NFL activation (IRS-1 phosphorylation) is accelerated by astrin deficiency. Treatment as in Figure 2B. See Figure S2A for relative quantitation of S6K1-T389.

(E) Astrin deficiency induces mTOR-raptor association in response to insulin/aa. Treatment as in Figure 2B. Nuclei stained with DAPI (blue); PLA performed for raptor and mTOR (red).

(F) Relative quantitation of mTORC1 assembly in situ in response to insulin/aa without and with astrin siRNA (E). Dots/cell were counted. Data represented as mean ± SEM.

Data representative of at least three independent experiments. See also Figure S2.

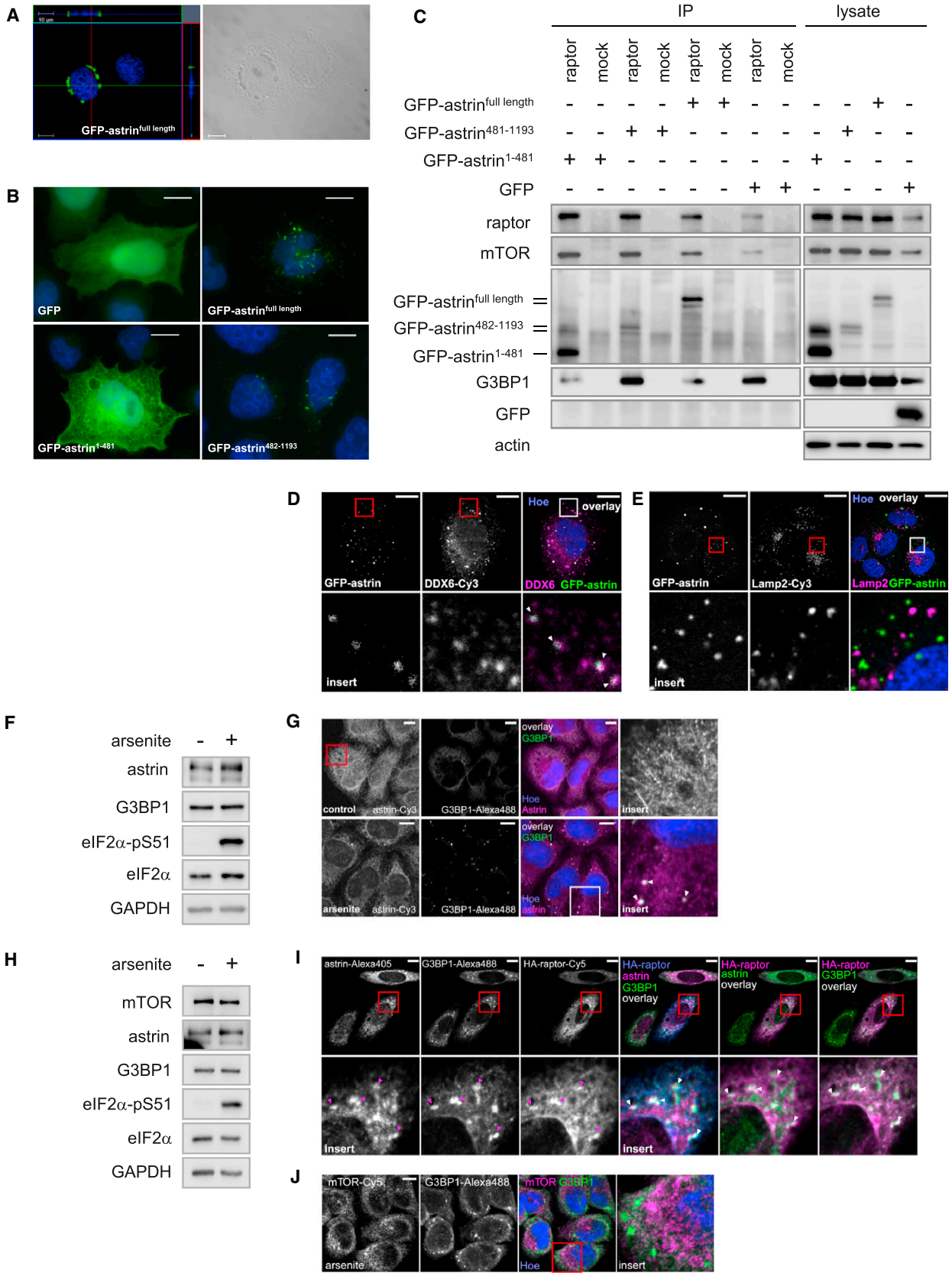

(legend on next page)

S6K1 phosphorylates IRS1-S636/639 to inhibit IRS1 (i.e., the NFL). In line with activated mTORC1 and S6K1 upon astrin deficiency, we found IRS1-pS636/639 induced by astrin siRNA (Figure 2C). Time course experiments upon insulin induction (Figure 2D) revealed that astrin deficiency accelerates the phosphorylation induction of the mTORC1 substrates S6K1-T389 and PRAS40-S183 (5 min after induction in siAstrin versus 7 min in control cells, respectively). siAstrin also accelerated the onset of the NFL (IRS1-pS636/639), resulting in suppression of S6K1-pT389 (decline at 7 min after induction in siAstrin cells, as compared to steady state induction up to 20 min after induction in control cells). PLA analysis revealed an initial drop of mTOR-raptor association, which remained low in control cells but increased in siAstrin cells from 5 min after induction on (Figures 2E and 2F).Thus, overall mTORC1 network dynamics are accelerated in the absence of astrin, and this correlates with an increase in mTOR-raptor association.

The Astrin-Raptor Complex Localizes to SGs

To address the cellular localization of the astrin-raptor complex we generated recombinant GFP-astrin fusion constructs. The modular structure of astrin with its N-terminal globular head domain and the two C-terminal coiled-coil domains (Gruber et al., 2002) led us to generate constructs for full-length astrin (GFP-astrin$^{\text{full length}}$), the N-terminal head domain (GFP-astrin$^{1\text{-}481}$), and the C-terminal coiled-coil domains (GFP-astrin$^{482\text{-}1193}$) (depicted in Figure S3A). GFP-astrin$^{\text{full length}}$ localized to cytoplasmic granular structures that were also visible by light microscopy (Figure 3A). Of note, C-terminal GFP-astrin$^{482\text{-}1193}$ localized to similar structures, whereas N-terminal GFP-astrin$^{1\text{-}481}$ showed a diffuse cytosolic localization (Figure 3B). GFP-astrin$^{\text{full length}}$ and N-terminal GFP-astrin$^{1\text{-}481}$ copurified with raptor, whereas C-terminal GFP-astrin$^{482\text{-}1193}$ only weakly associated with raptor (Figure 3C). This suggests that astrin's N-terminal head domain mediates primarily raptor binding, whereas astrin's C-terminal coiled-coil domains mediate mainly its localization.

The granular GFP-astrin assemblies resemble the patterns seen with overexpression of PB or SG components (Anderson and Kedersha, 2009). Being in constant exchange with each other, SGs and PBs share several components including the protein p54/DDX6. GFP-astrin$^{\text{full length}}$ (expression efficiency shown in Figure S3B) colocalized with p54/DDX6 (Figure 3D). The active mTOR-raptor complex localizes to lysosomes (Sancak et al., 2010). In contrast, GFP-astrin$^{\text{full length}}$ did not colocalize with the lysosomal marker Lamp2 (Figure 3E), strengthening the notion that mTOR and astrin bind raptor in a mutually exclusive manner.

To analyze whether endogenous astrin localizes to SGs upon stress, we treated cells with with arsenite (500 μM, 30 min). As reported, arsenite induced an inhibitory phosphorylation of the translation initiation factor eIF2α at S51 (Farny et al., 2009) (Figure 3F). The commercial astrin antibody used in this study detected GFP-astrin by immunofluorescence (IF) (Figure S3C), and it detected astrin in mitotic cells at the spindle (Figure S3D), corresponding to astrin's published localization (Thein et al., 2007). In nonstressed cells, endogenous astrin showed a microtubuli pattern (Figure 3G, top and insert), as reported (Mack and Compton, 2001). Upon arsenite the SG marker G3BP1 (Tourrière et al., 2003) localized to granular cytoplasmic structures, i.e., SGs, and astrin partially colocalized with G3BP1 (Figure 3G, bottom and insert). HA-raptor colocalized with astrin and G3BP1 upon arsenite (Figure 3I), whereas no colocalization in granular structures was observed in unstressed cells (Figure S3E). mTOR did not colocalize with G3BP1 upon arsenite treatment (Figure 3J; levels of all three proteins shown in Figure 3H). Thus, upon arsenite, astrin and raptor, but not mTOR, colocalize with SGs.

Does relocalization of the astrin-raptor complex to SGs under oxidative stress reduce mTOR-raptor association? To test this, we analyzed whether raptor binds G3BP1. G3BP1 associated with raptor in situ, which was increased by arsenite stress (Figures 4A, 4B, and S4A). We confirmed this finding by G3BP1-raptor co-IP (Figures 4C and S4B), which was induced by arsenite stress. Second, we tested astrin-G3BP1 association

Figure 3. Astrin and Raptor Relocalize to SGs upon Oxidative Stress

(A) GFP-astrin localizes into granular structures that are visible by light microscopy. GFP-astrin$^{\text{full length}}$ in HeLa cells was detected by confocal microscopy. Left: GFP-astrin (green) and Hoechst (blue). Cross-section through the horizontal and vertical plane. Right: light microscopy of granular GFP-astrin structures.

(B) The C-terminal coiled-coil domains of astrin mediate its distinct localization. GFP-astrin$^{\text{full length}}$, GFP-astrin$^{1\text{-}481}$, GFP-astrin$^{482\text{-}1193}$ (green), Hoechst (blue); detection by fluorescence microscopy.

(C) The N-terminal head domain of astrin binds to raptor. Cells expressing GFP-astrin$^{\text{full length}}$, GFP-astrin$^{1\text{-}481}$, GFP-astrin$^{482\text{-}1193}$, or GFP were used for raptor IPs.

(D) GFP-astrin colocalizes with the SG/PB marker p54/DDX6. GFP-astrin (green), p54/DDX6 (magenta), Hoechst (blue). Insert: blow-up of square. See Figure S3B for IB detection of GFP-astrin and p54/DDX6 expression.

(E) GFP-astrin does not colocalize with the lysosomal marker Lamp2. GFP-astrin (green), Lamp2 (magenta), Hoechst (blue). Insert: blow-up of square. See Figure S3B for IB detection of GFP-astrin expression.

(F) IB analysis of cells in (G) for astrin and G3BP1 expression, and oxidative stress induction (eIF2α-pS51).

(G) Astrin localizes under arsenite stress into G3BP1 positive SGs. HeLa cells cultivated in control and stress conditions (arsenite); astrin (magenta), G3BP1 (green), and Hoechst (blue). White arrows: astrin-G3BP1 colocalization.

(H) IB analysis of cells in (J) for mTOR, astrin, and G3BP1 expression and oxidative stress induction (eIF2α-pS51).

(I) HA-raptor colocalizes with astrin into G3BP1 positive SGs under arsenite stress. Columns 1–3: Cells transfected with HA-raptor, arsenite stressed, and stained against astrin, G3BP1, and HA. Insert: blow-up of square (points of colocalization: magenta arrow heads). Columns 4–6 (left to right): Triple overlay (white) of HA-raptor (blue), astrin (magenta), G3BP1 (green); double overlay (white) of astrin (green) and HA-raptor (magenta); double overlay (white) of G3BP1 (green) and HA-raptor (magenta). Insert: blow-up of square. See Figure S3E for control in unstressed cells.

(J) mTOR does not colocalize with astrin or G3BP1 under arsenite stress. Arsenite-stressed cells. mTOR (magenta), G3BP1 (green), with Hoechst (blue). Insert: blow-up of square.

Data representative of at least three independent experiments. See also Figure S3.

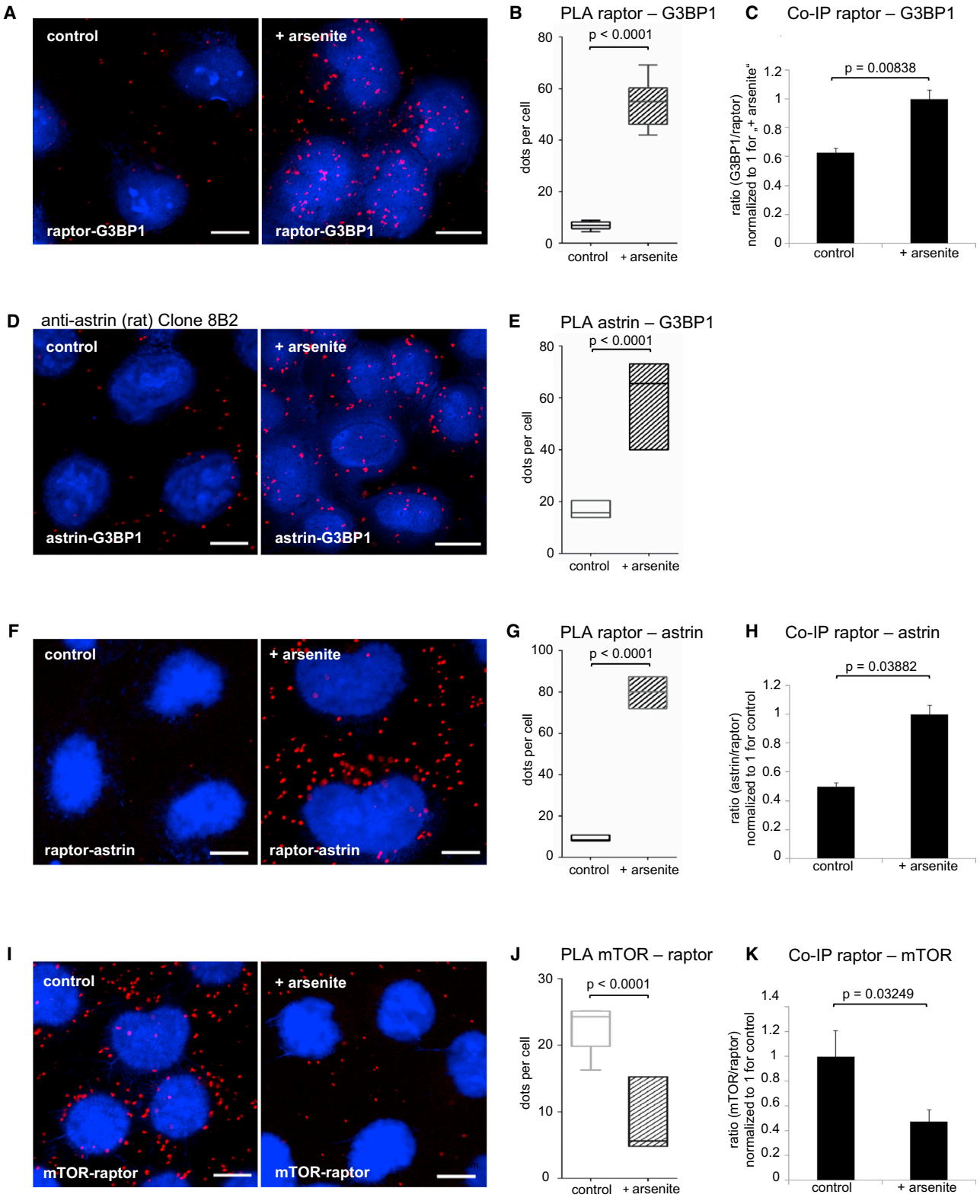

(legend on next page)

in situ, which was also increased by arsenite (Figures 4D, 4E, and S4C). We confirmed this result with an astrin antibody of different clonality (Figures S4D and S4E). Third, also astrin association with raptor was increased by arsenite in situ (Figures 4F, 4G, and S4F) and in co-IPs (Figure 4H and S4G). Thus, formation of the raptor-astrin complex and its association with SGs is induced by arsenite.

Astrin Inhibits mTOR-Raptor Association and Recruits Raptor to SGs

As astrin competes with mTOR for raptor binding (Figures 1E–1H), stress conditions that induce the astrin-raptor complex (Figures 4F–4H) may reduce mTORC1 levels. Indeed arsenite reduced raptor-mTOR association, in situ (Figures 4I and 4J) and in co-IPs (Figures 4K and S4B). This is in agreement with earlier studies (Sarbassov and Sabatini, 2005; Yoshida et al., 2011) reporting that oxidative stress disassembles mTORC1. We conclude that raptor-astrin association with SGs correlates with mTOR-raptor disassembly.

Is astrin responsible for raptor recruitment to SGs and for reduced mTOR-raptor association? Indeed, astrin inhibition under arsenite stress reduced raptor-G3BP1 association in co-IPs (Figures 5A and S5A) and in situ (Figures 5B, 5D, and S5B), and astrin knockdown induced the mTOR-raptor complex (Figures 5C, 5D and S5C). Thus, astrin is required for raptor recruitment to SGs.

We next tested whether these effects were also observable using another SG-inducing stressor. Hydrogen peroxide (H_2O_2) induces SGs (Emara et al., 2012). We repeated the above experiments with 2 mM H_2O_2, which reproduced the results obtained with arsenite (Figure 5D). We also further confirmed the astrin dependency of raptor-SG association by monitoring another SG marker, eukaryotic initiation factor 3 (eIF3) (Kedersha and Anderson, 2007) (Figures 5E and 5F). In agreement with the data for G3BP1 (Figures 5A, 5B, and 5D), arsenite induced raptor-eIF3 association, which was ablated by astrin knockdown (Figures 5E and 5F). We also analyzed which fraction of cellular raptor is bound to mTOR or astrin. We found by PLA that in control cells (Figures S5D and S5E) or arsenite stressed cells (Figures S5F, S5G–S5I) roughly one third of the cellular raptor molecules associated with mTOR or astrin, respectively, contributing to mTOR complex stoichiometry.

Astrin-Mediated Inhibition of mTORC1 under Stress Is SG Dependent

What is the function of astrin-mediated raptor recruitment to SGs? SG formation (Figure 6A) and G3BP1 expression (Figure 6B) still occurred in the absence of astrin. Also in raptor-deficient cells we did not detect an apparent reduction of SG formation (Figures 6C and 6D). Hence, under the conditions tested here, SG formation did not require astrin or mTORC1. Next, we analyzed whether astrin and SGs exert an inhibitory effect on mTORC1. Whereas loss of TSC1-TSC2 induces mTORC1 kinase activity upon stress (Yoshida et al., 2011), the here-observed mTOR-raptor dissociation may be a compensatory mechanism to prevent mTORC1 hyperactivation. In agreement with this hypothesis and published data (Wang and Proud, 1997), arsenite per se induced S6K1-T389 phosphorylation, which was inhibited by rapamycin (Figure 6E) or raptor shRNA (Figure 6F). Astrin inhibition further induced S6K1-T389 phosphorylation upon arsenite (Figure 6G) by 37% (Figure S6A), which was inhibited by PP242 (Figure 6H) or rapamycin (Figure S6B). Thus, astrin inhibition induces mTORC1 upon oxidative stress. A time course analysis revealed that astrin deficiency led to stronger and more sustained S6K1-pT389 induction, whereas stronger induction of the other mTORC1 substrate 4E-BP1-pT37/46 became apparent from 40 min after induction on (Figure 6I). This is in line with recent studies reporting that mTORC1 substrates respond to mTORC1 induction with differential context-dependent, temporal dynamics (Dennis et al., 2013; Rapley et al., 2011). We found that also heat shock, an alternative SG-inducing stress, led to enhanced S6K1-pT389 induction in astrin-deprived cells

Figure 4. Oxidative Stress Induces Astrin-Raptor Association in SGs and Reduces Raptor-mTOR association

(A) Raptor associates with G3BP1 in situ, and the association is induced by arsenite. DAPI (blue), and PLA for raptor and G3BP1 (red).

(B) Relative quantitation of (A), raptor-G3BP1 association without and with arsenite stress. Dots/cell counts. Data represented as median, 25^{th}–75^{th} percentile (box), 5^{th}–95^{th} percentile (whiskers). See Figure S4A for quantitation of fluorescence intensity.

(C) Relative quantitation of coimmunoprecipitated G3BP1 with raptor, without and with arsenite stress. IPs detected by IB (representative example in Figure S4B). G3BP1 signals quantified and normalized to the raptor signal for n = 3 experiments. G3BP1/raptor ratio set to 1 for arsenite treatment. Data represented as mean ± SEM.

(D) Astrin associates with G3BP1 in situ, and the interaction is induced by arsenite stress. DAPI (blue), PLA with anti-astrin antibody (rat, clone 8B2) and G3BP1 (red). See also Figures S4D and S4E.

(E) Relative quantitation of (D), astrin-G3BP1 association without and with arsenite stress. Dots/cell counts. Data represented as median, 25^{th}–75^{th} percentile (box), 5^{th}–95^{th} percentile (whiskers). See Figure S4C for quantitation of fluorescence intensity.

(F) Arsenite stress induces raptor-astrin association in situ. PLA for astrin and raptor (red); DAPI (blue).

(G) Relative quantitation of (F), raptor-astrin association without and with arsenite stress. Dots/cell counts. Data represented as median, 25^{th}–75^{th} percentile (box), 5^{th}–95^{th} percentile (whiskers). See Figure S4F for quantitation of fluorescence intensity.

(H) Astrin co-IP with raptor is induced upon arsenite stress. IPs detected by IB (representative example shown in Figure S4G). Astrin signals quantified and normalized to the raptor signal for n = 3 experiments. astrin/raptor ratio set to 1 for arsenite treatment. Data represented as mean ± SEM.

(I) Decreased raptor-mTOR (mTORC1) association in situ upon arsenite stress. PLA for mTOR and raptor (red); DAPI (blue).

(J) Relative quantitation of (I), raptor-mTOR (mTORC1) assembly. Dots/cell counts. Data represented as median, 25^{th}–75^{th} percentile (box), 5^{th}–95^{th} percentile (whiskers).

(K) mTOR co-IP with raptor (mTORC1) is reduced upon arsenite stress. IPs detected by IB (representative example shown in Figure S4B). mTOR signals quantified and normalized to the raptor signal for n = 3 experiments. mTOR/raptor ratio set to 1 for control treatment. Data represented as mean ± SEM.

Data representative of at least three independent experiments. See also Figure S4.

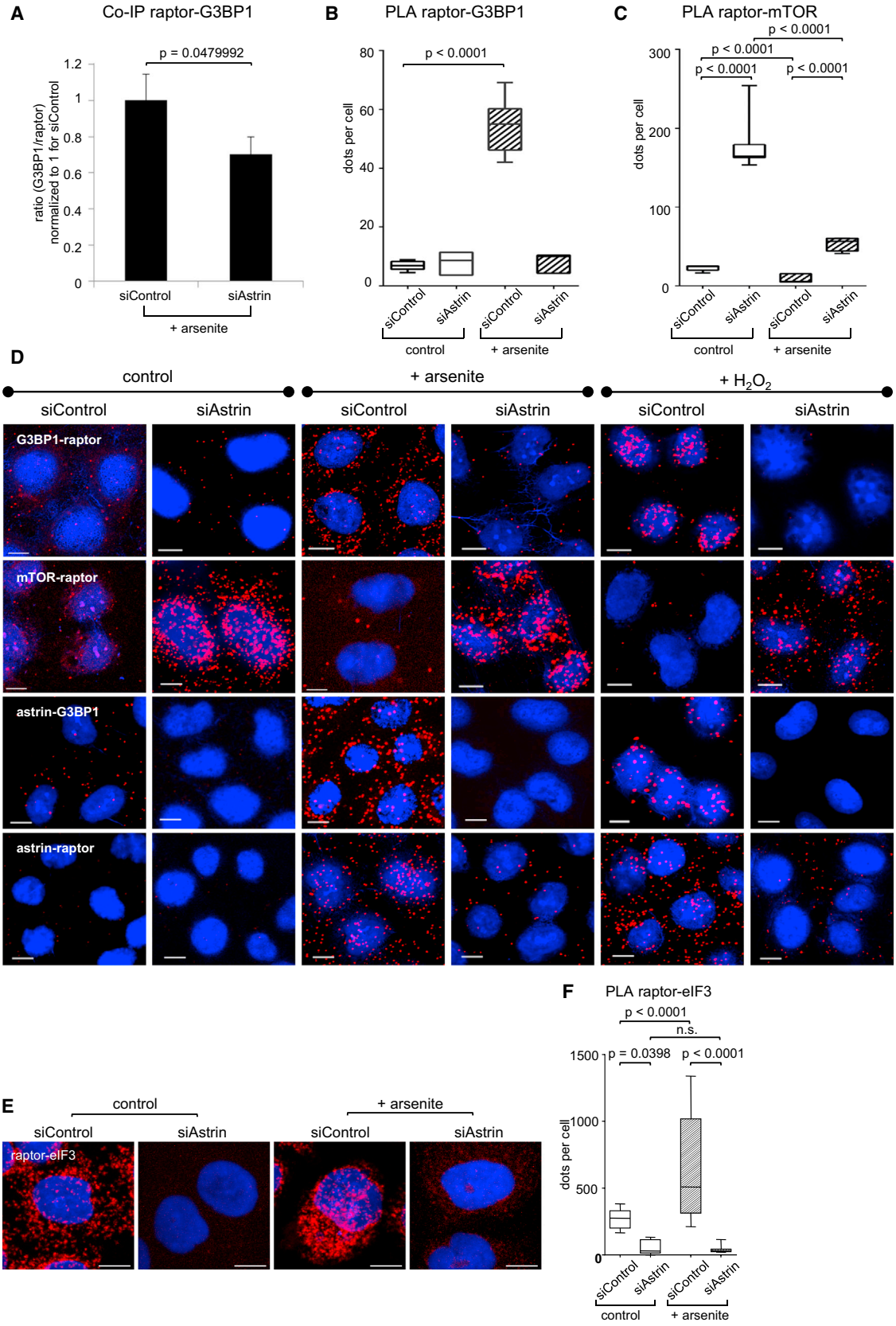

(legend on next page)

(Figure S6C). Thus, astrin prevents mTORC1 hyperactivation under conditions that induce SGs.

Because mTORC1 is active at lysosomes, we tested whether astrin affects raptor-Lamp2 association. Astrin knockdown induced raptor-Lamp2 association in control cells (Figures 6J and 6K), which was in line with mTORC1 induction by siAstrin under basal conditions or insulin/aa stimulation (Figures 2 and S2A). Arsenite decreased raptor-Lamp2 association, and this remained unchanged in siAstrin cells (Figures 6J and 6K). This finding is in agreement with a recent study reporting the loss of raptor-lysosome colocalization under stress (Wippich et al., 2013). Thus, mTORC1 under stress may be active at a site other than lysosomes, raising the possibility of a novel yet unknown mechanism of mTORC1 activation.

Does the inhibitory effect of astrin toward mTORC1 under stress require SGs? To test this, we combined arsenite stress with short term (30 min) cycloheximide (chx) treatment, which stalls mRNA in polysomes and inhibits SG assembly (Kedersha and Anderson, 2007). We confirmed this in our system by cotreating cells with arsenite and chx, followed by IF analysis of G3BP1 (Figure 7A). Next, we tested the effect of SG inhibition on mTORC1 activity. Chx combined with arsenite strongly induced S6K1-pT389, and under these conditions, shAstrin failed to further induce mTORC1 activity (Figure 7B). Chx alone after 30 min did not have a stimulating effect on mTORC1. We repeated the experiment with H_2O_2 and obtained similar results (Figures 7C, 7D, and S6A, right). Thus, prevention of mTORC1 hyperactivation by astrin under oxidative stress is SG dependent. In addition, we tested emetine, another translation inhibitor that stabilizes polysomes and thereby inhibits SGs (Kedersha et al., 2000) (Figures S7A and S7B). Like chx, also emetine further induced mTORC1 under oxidative stress in siControl but not in siAstrin cells. As chx and emetine not only inhibit SGs but also translation, we tested hippuristanol (Bordeleau et al., 2006) and puromycin (Kedersha et al., 2000), two translation inhibitors, which destabilize polysomes and thereby induce SG assembly (Anderson and Kedersha, 2008), for their effects on mTORC1 induction by shAstrin (Figures S7B, S7C, and S7D). Both hippuristanol and puromycin failed to further induce the mTORC1 readout S6K1-pT389 but rather inhibited mTORC1, ruling out that translational arrest alone induced mTORC1. It should be noted that astrin inhibition did not affect raptor levels and vice versa (Figure 7E), ruling out that altered raptor or astrin levels add to the observed effects. Thus, SGs are required for astrin's inhibitory effect on mTORC1, to restrict mTORC1 activation by oxidative stress.

SG and Astrin-Dependent mTORC1 Repression Protects Cancer Cells from Oxidative Stress-Induced Apoptosis

Redox stress is a common condition in tumors, and tumor cells need to evade apoptosis in response to oxidative insults (Fruehauf and Meyskens, 2007; Sosa et al., 2013). Of note, hyperactive mTORC1 signaling sensitizes cells to apoptosis (Shah et al., 2004; Lee et al., 2007), and astrin deficiency facilitates apoptosis (Gruber et al., 2002). Is enhanced apoptosis in astrin-deficient cells mediated by loss-of-astrin-induced mTORC1 hyperactivation? Indeed, siAstrin enhanced apoptosis in H_2O_2 treated HeLa cells, as measured by cleaved PARP (poly [ADP-ribose] polymerase) (Figure 7E). Apoptosis induced by loss of astrin was inhibited by shRaptor (Figure 7E). We conclude that mTORC1 activity restriction by astrin protects HeLa cells against apoptosis. Does this finding translate to other cancer cells? siAstrin facilitated PARP cleavage also in several breast cancer cell lines (Figure S7E). In MCF-7 breast cancer cells apoptosis sensitization by astrin deficiency was phenocopied by SG inhibition (Figure 7F), and mTORC1 inhibition prevented apoptosis in astrin-deficient cells (Figure 7G). SG inhibition by chx facilitated apoptosis, and under this condition, astrin depletion could not further enhance apoptosis (Figure 7F). Rapamycin suppressed apoptosis in siAstrin cells (Figure 7G). We confirmed this by live-cell imaging to determine the onset of apoptotic membrane blebbing (Wickman et al., 2012) (Figures 7H and 7I and Movies S1 and S2). Membrane blebbing occurred in siAstrin cells already at ca. 100 min after H_2O_2, as compared to 200 min in control cells (Figure 7H and Movie S1). Chx reduced blebbing onset in control cells to 100 min, whereas no further reduction was observed in siAstrin cells. In contrast, rapamycin delayed the mean onset of blebbing in siAstrin cells by 50 min (Figure 7I and Movie S2). Our data are consistent with a model in which astrin in a SG-dependent manner restricts mTORC1 activity to prevent mTORC1 hyperactivation and apoptosis upon oxidative stress. One mechanism for apoptosis suppression in cancer cells is Akt-mediated inhibition of the transcription factors FoxO1/3A (Myatt et al., 2011); Akt is inhibited by the mTORC1-dependent NFL. In line with this, we observed that mTORC1 inhibition by rapamycin-induced FoxO1/3A phosphorylation and repressed oxidative stress and siAstrin-induced apoptosis (Figure 7G). In summary, astrin inhibits apoptosis in cancer cells by preventing mTORC1 hyperactivation upon oxidative stress.

Figure 5. Astrin Is Required for Raptor Recruitment to SGs upon Redox Stress

(A) Astrin siRNA reduces raptor-G3BP1 co-IP under arsenite stress. IPs detected by IB (representative example shown in Figure S5A). G3BP1 signals quantified and normalized to the raptor signal for n = 3 experiments. G3BP1/raptor ratio set to 1 for control treatment. Data represented as mean ± SEM.

(B) Relative quantitation of (D), raptor-G3BP1 association without and with astrin siRNA and arsenite stress. Dots/cell counts. Data represented as median, 25^{th}–75^{th} percentile (box), 5^{th}–95^{th} percentile (whiskers). See Figure S5B for quantitation of fluorescence intensity.

(C) Relative quantitation of (D), combined arsenite and astrin siRNA effects on mTORC1 assembly (raptor-mTOR). Dots/cell counts. Data represented as median, 25^{th}–75^{th} percentile (box), 5^{th}–95^{th} percentile (whiskers). See Figure S5C for quantitation of fluorescence intensity.

(D) Oxidative stress induced by H_2O_2 reproduces the effects of arsenite stress on astrin-G3BP1, astrin-raptor, raptor-mTOR, and raptor-G3BP1 complexes without and with astrin siRNA. PLA (red); DAPI (blue).

(E) Astrin mediates raptor binding to the SG marker and translation initiation factor eIF3 in unstressed and arsenite-stressed cells. PLA (red); DAPI (blue).

(F) Relative quantitation of (E), raptor-eIF3 association without and with astrin siRNA and arsenite stress. Dots/cell counts. Data represented as median, 25^{th}–75^{th} percentile (box), 5^{th}–95^{th} percentile (whiskers).

Data representative of at least three independent experiments. See also Figure S5.

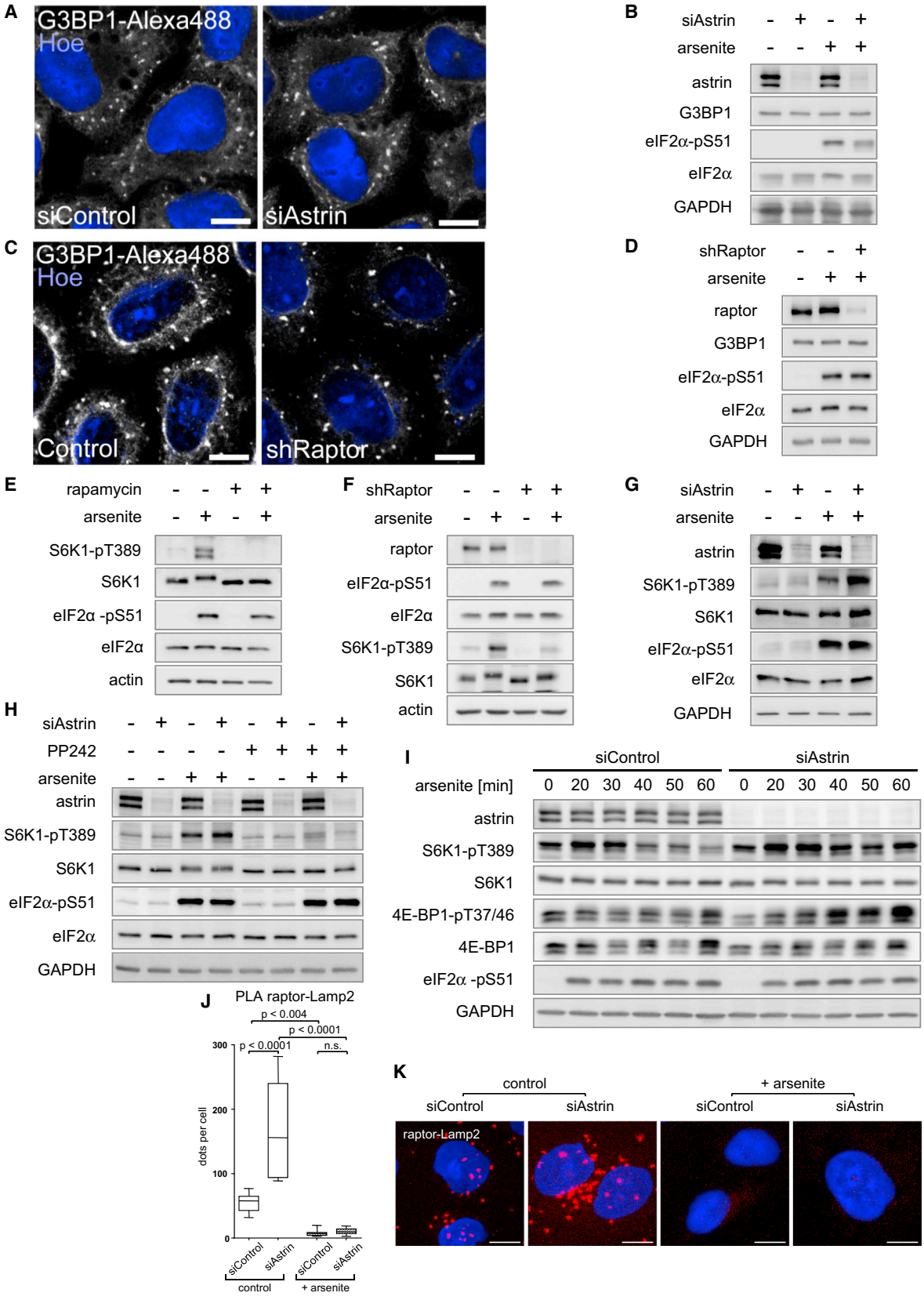

(legend on next page)

DISCUSSION

Wippich et al. (2013) recently reported that SGs inhibit mTORC1 via sequestration of mTORC1 components. In this study, we identify astrin as a molecular link enabling mTORC1 regulation by SGs under oxidative stress in mammalian cells (summarized in Figure 7J). Already a decade ago Kim et al. (2002) observed that conditions that inhibit the mTORC1 pathway correlate with a stronger mTOR-raptor association and vice versa. Our study reveals astrin as a key factor that inhibits mTORC1 association, and this mechanism restricts mTORC1 activity in metabolically challenged cells to prevent mTORC1 hyperactivation-induced apoptosis.

Redox activation of mTORC1 is mediated by inactivation of TSC1-TSC2, in a PI3K- and Akt-independent manner (Yoshida et al., 2011). Accordingly, we observed that mTORC1 induction by arsenite stress and mTORC1 hyperactivation by siAstrin still occurred when PI3K and Akt induction were inhibited (Figure S7F). Furthermore, TSC2 was downregulated upon arsenite stress, which correlated with induced S6K1-pT389 (Figure S7G). This supports TSC1-TSC2 inhibition as a transducer of activating redox signals to mTORC1. Consequently, another component, i.e., astrin, needs to take over as an mTORC1 inhibitor, so that the cell retains mTORC1 under control. Notably, we found that TSC2 deprivation induced astrin protein levels (Figure S7H). Therefore, TSC1-TSC2 suppression may not only induce mTORC1 in response to redox; but TSC1-TSC2 deficiency may also upregulate the levels of astrin thereby allowing to maintain mTORC1 in check.

Why does mTORC1 need to be active upon oxidative stress? Although overall cellular translation is reduced, proteins required for the cellular stress response need to be expressed (Yamasaki and Anderson, 2008). Translation under stress depends on upstream open reading frames (uORF) and internal ribosomal entry sites (IRES) (Holcik and Sonenberg, 2005). mTORC1 induces both IRES-mediated (Dai et al., 2011; Grzmil and Hemmings, 2012) and uORF-dependent translation (Ramírez-Valle et al., 2008), and both mTORC1 and SGs control translation of stress related factors (Buchan and Parker, 2009; Chou et al., 2012; Hsieh et al., 2012; Huo et al., 2012; Thoreen et al., 2012). Accordingly, we report that several stress related proteins (HSF1, hnRNP-A1, and Hsp70) require mTORC1 for their expression upon arsenite stress (Figure S7G). hnRNP-A1 mediates IRES-dependent translation in tumor cells (Rübsamen et al., 2012), whereas HSF1 mediates transcriptional events, including Hsp70 expression (Chou et al., 2012). In contrast, activating transcription factor ATF-4 (its mRNA containing two uORFs, Vattem and Wek, 2004) is repressed by mTORC1 under nonstress conditions, but constitutively expressed when raptor is absent (Figure S7G). Thus, mTORC1 differentially controls expression of stress related proteins.

One effect of astrin-mediated mTORC1 inhibition is the inactivation of the mTORC1-dependent NFL. In turn, Akt activation is well known to prevent apoptosis (Appenzeller-Herzog and Hall, 2012). In healthy cells astrin-mediated inhibition of apoptosis may be beneficial as it prevents cells from undergoing apoptosis upon transient stresses or metabolic challenge. In contrast, in cancer cells astrin-mediated mTORC1 and apoptosis suppression can become detrimental as it prevents overgrowing cells from undergoing apoptosis. Notably, astrin is highly expressed in tumor cells (Buechler, 2009; Välk et al., 2010) and spermatocytes (Shao et al., 2001). Hence, astrin inhibition may allow modulation of mTOR network activity specifically in tumor cells, opening new avenues to cancer therapy.

Of note, the growth factor insulin controls protein translation via SGs (Karimian Pour and Adeli, 2011), suggesting that SGs play a role beyond stress. Our data support a general role of SGs in so far as we have identified astrin as a raptor interactor in unstressed cells (Figure 1), astrin inhibition induces mTORC1 assembly in both stressed and unstressed cells (Figure 5D), and the integral SG component eIF3 binds raptor also in unstressed cells in an astrin-dependent manner (Figure 5E).

Two studies (Takahara and Maeda, 2012; Wippich et al., 2013) report association of TOR/mTOR itself with the late SG marker Pbp-1/PABP1 (Anderson and Kedersha, 2008). The early SG marker G3BP1 did not colocalize with mTOR in our study. Thus, mTORC1 regulation by SGs may involve mTOR at later stages of SG assembly. In contrast to our data (Figure 6C), Fournier et al. (2013) reported that mTORC1 positively controls SG formation. The authors used a low arsenite concentration that did not activate mTORC1, which may enable the observation of mTORC1-dependent SG assembly.

It has been suggested that astrin deficiency leads to mitotic delay, due to a defective spindle check point (Gruber et al., 2002; Thein et al., 2007). Notably, mitotic defects in

Figure 6. Astrin Inhibits mTORC1 under Oxidative Stress

(A) Astrin siRNA does not prevent SG assembly under oxidative stress. G3BP1 (white), Hoechst (blue).

(B) IB analysis of (A) for astrin siRNA efficiency, G3BP1 expression, and oxidative stress induction (eIF2α-pS51).

(C) Raptor shRNA does not prevent SG assembly under oxidative stress. G3BP1 (white); Hoechst (blue).

(D) IB analysis of (C) for raptor shRNA efficiency, G3BP1 expression, and oxidative stress induction (eIF2α-pS51).

(E) Arsenite stress induces phosphorylation of the mTORC1 substrate S6K1-T389, and the effect is inhibited by rapamycin.

(F) Raptor shRNA inhibits phosphorylation of S6K1-T389 under arsenite stress.

(G) Astrin siRNA further induces S6K1-T389 under arsenite stress. See Figure S6A for relative quantitation of S6K1-pT389.

(H) PP242 inhibits induction of S6K1-T389 by arsenite stress and astrin siRNA. See also Figure S6B.

(I) Astrin siRNA induces differential phosphorylation of the mTORC1 substrates S6K1-T389 and 4E-BP1-T37/46 under arsenite stress over time.

(J) Relative quantitation of (K), raptor-Lamp2 association without and with astrin siRNA and arsenite stress. Dots/cell counts. Data represented as median, 25^{th}–75^{th} percentile (box), 5^{th}–95^{th} percentile (whiskers).

(K) Astrin deficiency induces raptor association with the lysosomal marker Lamp2 in unstressed cells, and raptor-Lamp2 association is abolished upon arsenite stress. PLA (red) for Lamp2 and raptor; DAPI (blue).

Data representative of at least three independent experiments. See also Figure S6.

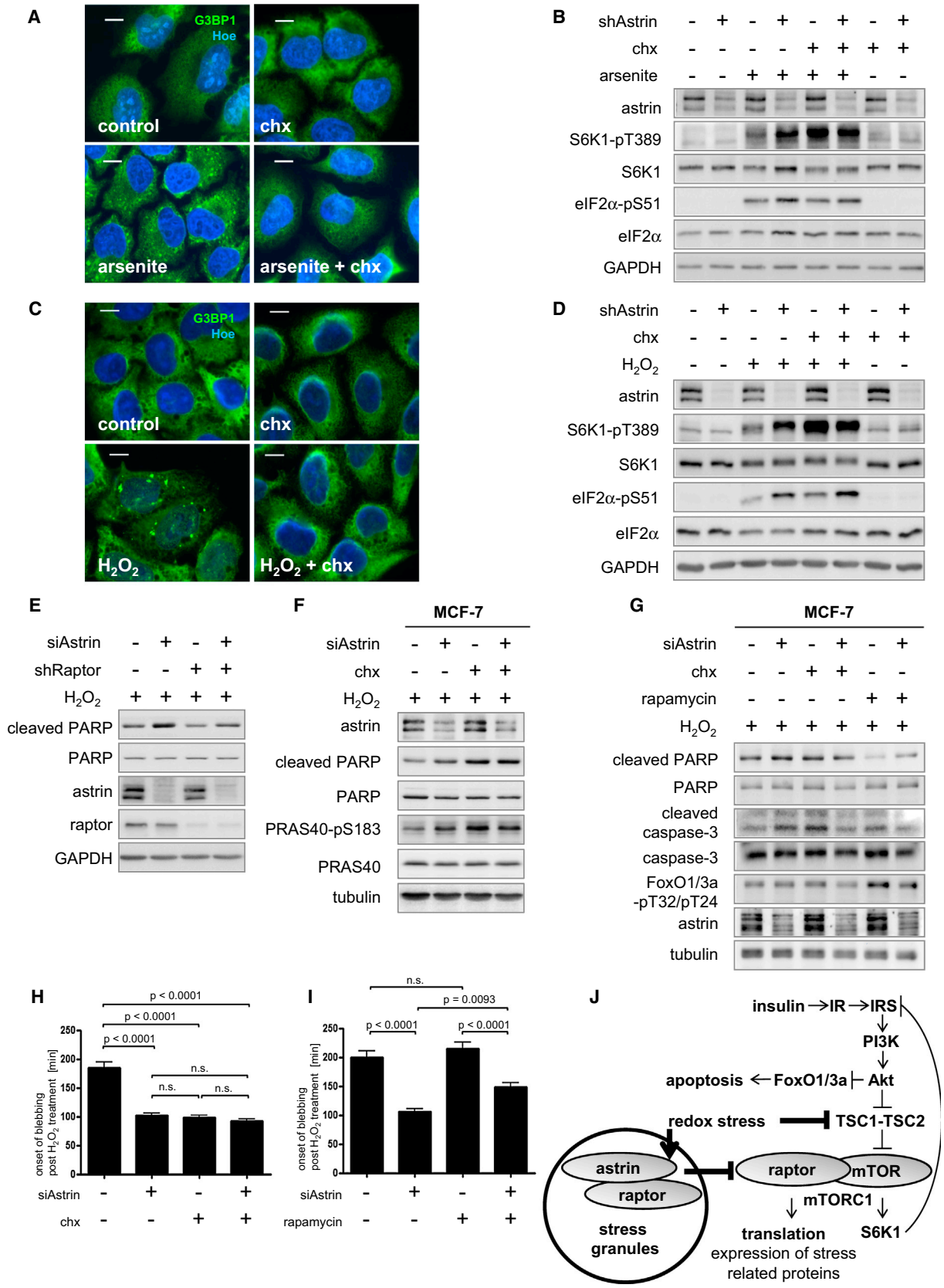

(legend on next page)

astrin-deficient cells are only detectable upon prolonged nocodazole treatment (Manning et al., 2010). Accordingly, and in line with others (Halim et al., 2013), we did not detect increased mitotic markers in nonsynchronized, astrin-deficient cells (Figure S2B). In turn, we observed mTORC1 induction by astrin knock down in nonsynchronized, but not in mitotic cells (Figure 2A). This suggests that astrin's effects on mitosis and on mTORC1 are two separate functions. This is underlined by our finding that G3BP1 binding to raptor is lost in cells arrested at G2/M by nocodazole or the Plk1 inhibitor GW 843682X (Figure S7I). We demonstrate in the present study that increased apoptosis in astrin-deficient cells can be suppressed by mTORC1 inhibition (Figure 7E, 7G, and 7I). Thus, our results unify and explain earlier reports on increased apoptosis upon astrin deficiency by showing that astrin-sensitive apoptosis is due to aberrant mTORC1 induction.

EXPERIMENTAL PROCEDURES

Cell Lines and Tissue Culture

Details on constructs and reagents can be found in the Extended Experimental Procedures. Insulin/aa induction was performed as described (Sonntag et al., 2012). Doxycycline (for shRNA induction) was removed over night prior to experiments. Prior to stress induction (500 μM arsenite or 2 mM H_2O_2), cells were starved for 16 hr in DMEM without glucose or fetal calf serum. SGs were analyzed after 30 min stress induction. Apoptosis was analyzed after 1–3 hr arsenite or H_2O_2. HeLa cells were synchronized with nocodazole (400 ng/ml) and subsequent mitotic shake off, and released as described (Thein et al., 2007).

Mass Spectrometry

Identification of novel mTOR and raptor interactors was performed as described (Thedieck et al., 2007).

Lysis, IP, and Immunoblotting

Lysis, IP, and immunoblotting (IB) were described elsewhere (Dalle Pezze et al., 2012;). See Extended Experimental Procedures for details on antibodies.

IF, Fluorescence Microscopy, and Confocal Microscopy

IF and PLA were performed as described (Thedieck et al., 2007; Thein et al., 2007; Söderberg et al., 2008). Scale bars are 10 μm. See Extended Experimental Procedures for detailed protocols.

Quantitations and Statistics

All experiments were performed in at least n = 3 replicates. Comparison of two groups was analyzed by nonparametrical two-tailed Student's t test assuming unequal variances. For multiple groups, statistical significance was analyzed by 1-way ANOVA. See Extended Experimental Procedures for details.

SUPPLEMENTAL INFORMATION

Supplemental Information includes Extended Experimental Procedures, seven figures, and two movies and can be found with this article online at http://dx.doi.org/10.1016/j.cell.2013.07.031.

ACKNOWLEDGMENTS

We thank Daryl P. Shanley (Newcastle University, UK) and Anna Johann for helpful discussions and critical reading of the manuscript. We thank Jerry Pelletier, McGill University, Montreal, Quebec, Canada for kindly providing hippuristanol. We thank our reviewers for excellent feedback and helpful experimental suggestions. Special thanks go to the staff of the Life Imaging Center (LIC) in the Center for Systems Biology, Albert-Ludwigs-University Freiburg for excellent confocal and widefield microscopy resources and the support in image analysis. This study was supported in part by the EC 6th FP NoE LifeSpan (LSHG-CT-2007-036894, to K.T. and R.B.), the Schlieben-Lange-Programm (K.T.), the Excellence Initiative of the German Research Foundation (EXC 294 to K.T., R.B., M.R., E.W.K., and R.N.; GSC-4, Spemann Graduate School to M.T.P.), the DFG Research Training Group RTG 1104 (S.R.), DFG grant KU 1504 (E.W.K.), BMBF Gerontosys II–NephAge (031 5896A) (K.T. and R.B.), the DFG grants CRC746 (M.R. and R.B.) and CRC850 (R.B.), the Freiburg Institute for Advanced Studies, FRIAS (K.T.), and the Peter und Traudl Engelhorn Stiftung zur Förderung der Biotechnologie und Gentechnik (K.T.). SNG is supported by an Addison Wheeler Fellowship. J.W.J. is supported by grants from the European Research Council (IRG-277169), Human Frontier Science Program (CDA00013/2011-C), the Netherlands Organization for Scientific Research (VIDI grant 016.126.338), the Dutch Digestive Foundation (grant WO 11-67), and the Dutch Diabetes Foundation (grant 2012.00.1537). A part of this work is the basis for a pending European patent application, filed on January 11, 2013 (Application no. EP13151022.4).

Received: January 9, 2013
Revised: April 3, 2013
Accepted: July 23, 2013
Published: August 15, 2013

REFERENCES

Alexander, A., Cai, S.L., Kim, J., Nanez, A., Sahin, M., MacLean, K.H., Inoki, K., Guan, K.L., Shen, J., Person, M.D., et al. (2010). ATM signals to TSC2 in the cytoplasm to regulate mTORC1 in response to ROS. Proc. Natl. Acad. Sci. USA *107*, 4153–4158.

Figure 7. SGs Are Required for mTORC1 Inhibition by Astrin under Oxidative Stress, and SG and Astrin-Dependent mTORC1 Repression Protects Cells from Oxidative Stress-Induced Apoptosis

(A) Cycloheximide (chx) prevents arsenite-induced SG formation. Fluorescence microscopy, G3BP1 (green), Hoechst (blue).
(B) Chx suppresses the astrin shRNA effect on S6K1-pT389 induction under arsenite stress.
(C) Chx prevents H_2O_2-induced SG formation. Fluorescence microscopy, G3BP1 (green), Hoechst (blue).
(D) Chx suppresses the astrin shRNA effect on S6K1-pT389 induction under H_2O_2 stress.
(E) siAstrin sensitizes cells to apoptosis, which is prevented by mTORC1 inhibition. HeLa cells, cleaved PARP = apoptosis marker.
(F) siAstrin sensitizes breast cancer cells to apoptosis in the presence but not in the absence of SGs. MCF-7 cells, cleaved PARP = apoptosis marker. See also Figure S7E.
(G) siAstrin sensitizes breast cancer cells to mTORC1-dependent apoptosis. MCF-7 cells; cleaved PARP, cleaved caspase-3 = apoptosis markers.
(H) siAstrin leads to early onset of apoptosis in the presence but not in the absence of SGs. MCF-7 cells analyzed by live-cell imaging; mean time point of blebbing onset indicated. Data represented as mean ± SEM. See also Movie S1.
(I) Early onset of apoptosis in siAstrin cells is suppressed by mTORC1 inhibition (rapamycin). MCF-7 cells analyzed by life cell imaging; mean time point of blebbing onset indicated. Data represented as mean ± SEM. See also Movie S2.
(J) Schematic representation of astrin- and SG-mediated mTORC1 inhibition and apoptosis suppression.
Data representative of at least three independent experiments. See also Figure S7.

Anderson, P., and Kedersha, N. (2008). Stress granules: the Tao of RNA triage. Trends Biochem. Sci. *33*, 141–150.

Anderson, P., and Kedersha, N. (2009). RNA granules: post-transcriptional and epigenetic modulators of gene expression. Nat. Rev. Mol. Cell Biol. *10*, 430–436.

Appenzeller-Herzog, C., and Hall, M.N. (2012). Bidirectional crosstalk between endoplasmic reticulum stress and mTOR signaling. Trends Cell Biol. *22*, 274–282.

Arimoto, K., Fukuda, H., Imajoh-Ohmi, S., Saito, H., and Takekawa, M. (2008). Formation of stress granules inhibits apoptosis by suppressing stress-responsive MAPK pathways. Nat. Cell Biol. *10*, 1324–1332.

Bae, G.U., Seo, D.W., Kwon, H.K., Lee, H.Y., Hong, S., Lee, Z.W., Ha, K.S., Lee, H.W., and Han, J.W. (1999). Hydrogen peroxide activates p70(S6k) signaling pathway. J. Biol. Chem. *274*, 32596–32602.

Benjamin, D., Colombi, M., Moroni, C., and Hall, M.N. (2011). Rapamycin passes the torch: a new generation of mTOR inhibitors. Nat. Rev. Drug Discov. *10*, 868–880.

Bordeleau, M.E., Mori, A., Oberer, M., Lindqvist, L., Chard, L.S., Higa, T., Belsham, G.J., Wagner, G., Tanaka, J., and Pelletier, J. (2006). Functional characterization of IRESes by an inhibitor of the RNA helicase eIF4A. Nat. Chem. Biol. *2*, 213–220.

Buchan, J.R., and Parker, R. (2009). Eukaryotic stress granules: the ins and outs of translation. Mol. Cell *36*, 932–941.

Buechler, S. (2009). Low expression of a few genes indicates good prognosis in estrogen receptor positive breast cancer. BMC Cancer *9*, 243.

Chang, M.S., Huang, C.J., Chen, M.L., Chen, S.T., Fan, C.C., Chu, J.M., Lin, W.C., and Yang, Y.C. (2001). Cloning and characterization of hMAP126, a new member of mitotic spindle-associated proteins. Biochem. Biophys. Res. Commun. *287*, 116–121.

Chou, S.D., Prince, T., Gong, J., and Calderwood, S.K. (2012). mTOR is essential for the proteotoxic stress response, HSF1 activation and heat shock protein synthesis. PLoS ONE *7*, e39679.

Dai, N., Rapley, J., Angel, M., Yanik, M.F., Blower, M.D., and Avruch, J. (2011). mTOR phosphorylates IMP2 to promote IGF2 mRNA translation by internal ribosomal entry. Genes Dev. *25*, 1159–1172.

Dalle Pezze, P., Sonntag, A.G., Thien, A., Prentzell, M.T., Gödel, M., Fischer, S., Neumann-Haefelin, E., Huber, T.B., Baumeister, R., Shanley, D.P., and Thedieck, K. (2012). A dynamic network model of mTOR signaling reveals TSC-independent mTORC2 regulation. Sci. Signal. *5*, ra25.

Dennis, M.D., Kimball, S.R., and Jefferson, L.S. (2013). Mechanistic target of rapamycin complex 1 (mTORC1)-mediated phosphorylation is governed by competition between substrates for interaction with raptor. J. Biol. Chem. *288*, 10–19.

Emara, M.M., Fujimura, K., Sciaranghella, D., Ivanova, V., Ivanov, P., and Anderson, P. (2012). Hydrogen peroxide induces stress granule formation independent of eIF2α phosphorylation. Biochem. Biophys. Res. Commun. *423*, 763–769.

Farny, N.G., Kedersha, N.L., and Silver, P.A. (2009). Metazoan stress granule assembly is mediated by P-eIF2alpha-dependent and -independent mechanisms. RNA *15*, 1814–1821.

Fournier, M.J., Coudert, L., Mellaoui, S., Adjibade, P., Gareau, C., Côté, M.F., Sonenberg, N., Gaudreault, R.C., and Mazroui, R. (2013). Inactivation of the mTORC1-eukaryotic translation initiation factor 4E pathway alters stress granule formation. Mol. Cell. Biol. *33*, 2285–2301.

Fruehauf, J.P., and Meyskens, F.L., Jr. (2007). Reactive oxygen species: a breath of life or death? Clin. Cancer Res. *13*, 789–794.

Gruber, J., Harborth, J., Schnabel, J., Weber, K., and Hatzfeld, M. (2002). The mitotic-spindle-associated protein astrin is essential for progression through mitosis. J. Cell Sci. *115*, 4053–4059.

Grzmil, M., and Hemmings, B.A. (2012). Translation regulation as a therapeutic target in cancer. Cancer Res. *72*, 3891–3900.

Gwinn, D.M., Asara, J.M., and Shaw, R.J. (2010). Raptor is phosphorylated by cdc2 during mitosis. PLoS ONE *5*, e9197.

Halim, V.A., Alvarez-Fernández, M., Xu, Y.J., Aprelia, M., van den Toorn, H.W., Heck, A.J., Mohammed, S., and Medema, R.H. (2013). Comparative phosphoproteomic analysis of checkpoint recovery identifies new regulators of the DNA damage response. Sci. Signal. *6*, rs9.

Holcik, M., and Sonenberg, N. (2005). Translational control in stress and apoptosis. Nat. Rev. Mol. Cell Biol. *6*, 318–327.

Hsieh, A.C., Liu, Y., Edlind, M.P., Ingolia, N.T., Janes, M.R., Sher, A., Shi, E.Y., Stumpf, C.R., Christensen, C., Bonham, M.J., et al. (2012). The translational landscape of mTOR signalling steers cancer initiation and metastasis. Nature *485*, 55–61.

Huang, C., Li, J., Ke, Q., Leonard, S.S., Jiang, B.H., Zhong, X.S., Costa, M., Castranova, V., and Shi, X. (2002). Ultraviolet-induced phosphorylation of p70(S6K) at Thr(389) and Thr(421)/Ser(424) involves hydrogen peroxide and mammalian target of rapamycin but not Akt and atypical protein kinase C. Cancer Res. *62*, 5689–5697.

Huo, Y., Iadevaia, V., Yao, Z., Kelly, I., Cosulich, S., Guichard, S., Foster, L.J., and Proud, C.G. (2012). Stable isotope-labelling analysis of the impact of inhibition of the mammalian target of rapamycin on protein synthesis. Biochem. J. *444*, 141–151.

Karimian Pour, N., and Adeli, K. (2011). Insulin silences apolipoprotein B mRNA translation by inducing intracellular traffic into cytoplasmic RNA granules. Biochemistry *50*, 6942–6950.

Kedersha, N., and Anderson, P. (2007). Mammalian stress granules and processing bodies. Methods Enzymol. *431*, 61–81.

Kedersha, N., Cho, M.R., Li, W., Yacono, P.W., Chen, S., Gilks, N., Golan, D.E., and Anderson, P. (2000). Dynamic shuttling of TIA-1 accompanies the recruitment of mRNA to mammalian stress granules. J. Cell Biol. *151*, 1257–1268.

Kim, D.H., Sarbassov, D.D., Ali, S.M., King, J.E., Latek, R.R., Erdjument-Bromage, H., Tempst, P., and Sabatini, D.M. (2002). mTOR interacts with raptor to form a nutrient-sensitive complex that signals to the cell growth machinery. Cell *110*, 163–175.

Laplante, M., and Sabatini, D.M. (2012). mTOR signaling in growth control and disease. Cell *149*, 274–293.

Lee, C.H., Inoki, K., Karbowniczek, M., Petroulakis, E., Sonenberg, N., Henske, E.P., and Guan, K.L. (2007). Constitutive mTOR activation in TSC mutants sensitizes cells to energy starvation and genomic damage via p53. EMBO J. *26*, 4812–4823.

Li, M., Zhao, L., Liu, J., Liu, A., Jia, C., Ma, D., Jiang, Y., and Bai, X. (2010). Multi-mechanisms are involved in reactive oxygen species regulation of mTORC1 signaling. Cell. Signal. *22*, 1469–1476.

Luo, X., Talarek, N., and De Virgilio, C. (2011). Initiation of the yeast G0 program requires Igo1 and Igo2, which antagonize activation of decapping of specific nutrient-regulated mRNAs. RNA Biol. *8*, 14–17.

Mack, G.J., and Compton, D.A. (2001). Analysis of mitotic microtubule-associated proteins using mass spectrometry identifies astrin, a spindle-associated protein. Proc. Natl. Acad. Sci. USA *98*, 14434–14439.

Manning, A.L., Bakhoum, S.F., Maffini, S., Correia-Melo, C., Maiato, H., and Compton, D.A. (2010). CLASP1, astrin and Kif2b form a molecular switch that regulates kinetochore-microtubule dynamics to promote mitotic progression and fidelity. EMBO J. *29*, 3531–3543.

Mihaylova, M.M., and Shaw, R.J. (2011). The AMPK signalling pathway coordinates cell growth, autophagy and metabolism. Nat. Cell Biol. *13*, 1016–1023.

Myatt, S.S., Brosens, J.J., and Lam, E.W. (2011). Sense and sensitivity: FOXO and ROS in cancer development and treatment. Antioxid. Redox Signal. *14*, 675–687.

Nakashima, A., Maruki, Y., Imamura, Y., Kondo, C., Kawamata, T., Kawanishi, I., Takata, H., Matsuura, A., Lee, K.S., Kikkawa, U., et al. (2008). The yeast Tor signaling pathway is involved in G2/M transition via polo-kinase. PLoS ONE *3*, e2223.

Polak, P., and Hall, M.N. (2009). mTOR and the control of whole body metabolism. Curr. Opin. Cell Biol. *21*, 209–218.

Ramírez-Valle, F., Braunstein, S., Zavadil, J., Formenti, S.C., and Schneider, R.J. (2008). eIF4GI links nutrient sensing by mTOR to cell proliferation and inhibition of autophagy. J. Cell Biol. *181*, 293–307.

Ramírez-Valle, F., Badura, M.L., Braunstein, S., Narasimhan, M., and Schneider, R.J. (2010). Mitotic raptor promotes mTORC1 activity, G(2)/M cell cycle progression, and internal ribosome entry site-mediated mRNA translation. Mol. Cell. Biol. *30*, 3151–3164.

Rapley, J., Oshiro, N., Ortiz-Vega, S., and Avruch, J. (2011). The mechanism of insulin-stimulated 4E-BP protein binding to mammalian target of rapamycin (mTOR) complex 1 and its contribution to mTOR complex 1 signaling. J. Biol. Chem. *286*, 38043–38053.

Rübsamen, D., Blees, J.S., Schulz, K., Döring, C., Hansmann, M.L., Heide, H., Weigert, A., Schmid, T., and Brüne, B. (2012). IRES-dependent translation of egr2 is induced under inflammatory conditions. RNA *18*, 1910–1920.

Sancak, Y., Bar-Peled, L., Zoncu, R., Markhard, A.L., Nada, S., and Sabatini, D.M. (2010). Ragulator-Rag complex targets mTORC1 to the lysosomal surface and is necessary for its activation by amino acids. Cell *141*, 290–303.

Sarbassov, D.D., and Sabatini, D.M. (2005). Redox regulation of the nutrient-sensitive raptor-mTOR pathway and complex. J. Biol. Chem. *280*, 39505–39509.

Sarbassov, D.D., Ali, S.M., Sengupta, S., Sheen, J.H., Hsu, P.P., Bagley, A.F., Markhard, A.L., and Sabatini, D.M. (2006). Prolonged rapamycin treatment inhibits mTORC2 assembly and Akt/PKB. Mol. Cell *22*, 159–168.

Shah, O.J., Wang, Z., and Hunter, T. (2004). Inappropriate activation of the TSC/Rheb/mTOR/S6K cassette induces IRS1/2 depletion, insulin resistance, and cell survival deficiencies. Curr. Biol. *14*, 1650–1656.

Shao, X., Xue, J., and van der Hoorn, F.A. (2001). Testicular protein Spag5 has similarity to mitotic spindle protein Deepest and binds outer dense fiber protein Odf1. Mol. Reprod. Dev. *59*, 410–416.

Söderberg, O., Leuchowius, K.J., Gullberg, M., Jarvius, M., Weibrecht, I., Larsson, L.G., and Landegren, U. (2008). Characterizing proteins and their interactions in cells and tissues using the in situ proximity ligation assay. Methods *45*, 227–232.

Sonntag, A.G., Dalle Pezze, P., Shanley, D.P., and Thedieck, K. (2012). A modelling-experimental approach reveals insulin receptor substrate (IRS)-dependent regulation of adenosine monosphosphate-dependent kinase (AMPK) by insulin. FEBS J. *279*, 3314–3328.

Sosa, V., Moliné, T., Somoza, R., Paciucci, R., Kondoh, H., and LLeonart, M.E. (2013). Oxidative stress and cancer: an overview. Ageing Res. Rev. *12*, 376–390.

Takahara, T., and Maeda, T. (2012). Transient sequestration of TORC1 into stress granules during heat stress. Mol. Cell *47*, 242–252.

Talarek, N., Cameroni, E., Jaquenoud, M., Luo, X., Bontron, S., Lippman, S., Devgan, G., Snyder, M., Broach, J.R., and De Virgilio, C. (2010). Initiation of the TORC1-regulated G0 program requires Igo1/2, which license specific mRNAs to evade degradation via the 5′-3′ mRNA decay pathway. Mol. Cell *38*, 345–355.

Thedieck, K., Polak, P., Kim, M.L., Molle, K.D., Cohen, A., Jenö, P., Arrieumerlou, C., and Hall, M.N. (2007). PRAS40 and PRR5-like protein are new mTOR interactors that regulate apoptosis. PLoS ONE *2*, e1217.

Thein, K.H., Kleylein-Sohn, J., Nigg, E.A., and Gruneberg, U. (2007). Astrin is required for the maintenance of sister chromatid cohesion and centrosome integrity. J. Cell Biol. *178*, 345–354.

Thomas, M.G., Loschi, M., Desbats, M.A., and Boccaccio, G.L. (2011). RNA granules: the good, the bad and the ugly. Cell. Signal. *23*, 324–334.

Thoreen, C.C., Chantranupong, L., Keys, H.R., Wang, T., Gray, N.S., and Sabatini, D.M. (2012). A unifying model for mTORC1-mediated regulation of mRNA translation. Nature *485*, 109–113.

Tourrière, H., Chebli, K., Zekri, L., Courselaud, B., Blanchard, J.M., Bertrand, E., and Tazi, J. (2003). The RasGAP-associated endoribonuclease G3BP assembles stress granules. J. Cell Biol. *160*, 823–831.

Välk, K., Vooder, T., Kolde, R., Reintam, M.A., Petzold, C., Vilo, J., and Metspalu, A. (2010). Gene expression profiles of non-small cell lung cancer: survival prediction and new biomarkers. Oncology *79*, 283–292.

Vattem, K.M., and Wek, R.C. (2004). Reinitiation involving upstream ORFs regulates ATF4 mRNA translation in mammalian cells. Proc. Natl. Acad. Sci. USA *101*, 11269–11274.

Wang, X., and Proud, C.G. (1997). p70 S6 kinase is activated by sodium arsenite in adult rat cardiomyocytes: roles for phosphatidylinositol 3-kinase and p38 MAP kinase. Biochem. Biophys. Res. Commun. *238*, 207–212.

Wickman, G., Julian, L., and Olson, M.F. (2012). How apoptotic cells aid in the removal of their own cold dead bodies. Cell Death Differ. *19*, 735–742.

Wippich, F., Bodenmiller, B., Trajkovska, M.G., Wanka, S., Aebersold, R., and Pelkmans, L. (2013). Dual specificity kinase DYRK3 couples stress granule condensation/dissolution to mTORC1 signaling. Cell *152*, 791–805.

Yamasaki, S., and Anderson, P. (2008). Reprogramming mRNA translation during stress. Curr. Opin. Cell Biol. *20*, 222–226.

Yoshida, S., Hong, S., Suzuki, T., Nada, S., Mannan, A.M., Wang, J., Okada, M., Guan, K.L., and Inoki, K. (2011). Redox regulates mammalian target of rapamycin complex 1 (mTORC1) activity by modulating the TSC1/TSC2-Rheb GTPase pathway. J. Biol. Chem. *286*, 32651–32660.